

Research Article

Characterization of CdTe Nanorods Visible Photoconductive Detector

Asama N.Naje^{†*} and Fatima Amer[†]

[†]University of Baghdad, Collage of Science, department of physics, Baghdad, Iraq

Accepted 20 March 2016, Available online 23 March 2016, Vol.6, No.2 (April 2016)

Abstract

CdTe nanorods are grown with varying reaction time period from (1-3h). The samples are characterized structurally and optically. A decrease in band gap is observed with increase the reaction time period. CdTe nanorods visible photoconductive detector films have been prepared on n-type porous silicon (PS) layer with etching time 10 min. The crystalline structure appears Hexagonal when the samples annealed under vacuum at 400°C for 1h. The Hall measurements show that all samples were p-type semiconductor. The response time of the fabricated CdTe/PS detector was measured by illuminating the samples visible light (Halogen lamp) and its values were increased from 52.2μs for 1hour to 0.378ms for 3 hours, the responsivity of the detector was decreased from 0.61A/W to 0.19 A/W and the highest specific detectivity was found to be $6.94 \times 10^{11} W^{-1} Hz^{1/2} cm$ for 2hours reaction time.

Keywords: CdTe nanorods, visible photoconductive detector, response time, responsivity.

1. Introduction

Over the past years, many advances have been made toward the synthesis of colloidal semiconductor nanorods and nanowires with diameters small enough to produce a quantum confinement of charge carriers (Y. Volkov *et al.*, 2005). Such confinement permits free-electron behavior in only one direction, along the length of the rod and therefore improved electronic transport can be achieved compared to that of semiconductor quantum dots, and thus it had widely used in serving as functional building blocks for photovoltaic and optoelectronic nanodevices (Y. Volkov *et al.*, 2005; X.N. Wang *et al.*, 2010). Cadmium telluride is considered as one of the most promising material due to the great tenability of its electro-optical properties that achieved by quantum confinement. It has a high absorption coefficient in the visible range and its band gap about 1.5 eV makes it optimum photovoltaic material (S. Suresh, 2014). CdTe has been synthesized in a various shapes and sizes by different methods like electrochemical deposition (R.S. Kapadnis *et al.*, 2013; M.C. Kum *et al.*, 2008), laser ablation (A.A. Ruth and J.A. Young, 2006) or chemical way including the wet chemical routs that has two different methods, the first way is to replace the surface-capping molecules on the particles prepared by the TOPO (trioctylphosphine oxide) method (D.V. Talapin *et al.*, 2002). The second method is to directly synthesize semiconductor nanoparticles in aqueous solution using stabilizers (capping ligands) such as Thiols (Y. Liu *et al.*, 2006) like in reports (Y. Shan *et al.*,

2014; S. Ananthakumar *et al.*, 2014; A.L. Rogach, 2000; M.S. Abd El-Sadek and S.M. Babu, 2010; Y. Wang *et al.*, 2013). Organic capping ligands allow for growth of nanoparticles while are stabilized against aggregation, they also influence solubility, size, shape, their surface charge, and their ability to adhere to substrates, which may affect the deposition of films of nanocrystals (W.Wang *et al.*, 2007; Y. Zahang and A. Clapp, 2011).

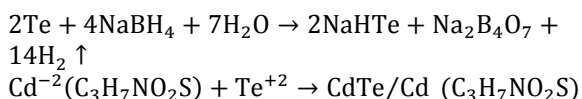
Photoconductive devices are attractive as highly sensitive photodetectors because of the large gain, which is defined as the number of collected charges per absorbed photon (H. Wei *et al.*, 2015). In this work, synthesize Cysteine-CdTe nanorods by wet chemical aqueous route and characterized by XRD and SEM also UV-visible spectrum was studied. CdTe nanorods layer was deposited on porous silicon to fabricate a visible photoconductive detector.

2. Procedure

Hydrous CdCl₂.H₂O (molecular weight-201.32gm/mole), Tellurium powder (molecular weight-127.6gm/mole) and NaBH₄ (molecular weight-37.83 gm/mole) have been taken to prepare different samples. L-Cysteine (C₃H₇NO₂S) has been used as a capping agent. Sodium borohydride has been taken to initiate the reaction at 60°C. In order to prepare different samples, the amounts of L-cysteine, CdCl₂, Te and NaBH₄ were taken in the ratios of 4:2:1:2. The reaction of Te powder with NaBH₄ and 3ml of distilled water was used as tellurium ions source in a dark violet solution of NaHTe. The precursor CdCl₂.H₂O was dissolved in 25ml of water, followed by adjusting the

*Corresponding author: Asama N.Naje

pH to the appropriate value (10.6) by drop wise addition of 1M solution of NaOH, and an appropriate amount of the stabilizer (L-cysteine) was added under stirring. The solution is placed in a three-necked flask fitted with a septum and valves and is aerated by Argon gas bubbling for 30 min at 60°C, the NaHTe solution added to the CdCl₂.H₂O solution. CdTe precursors are formed at this stage, which is accompanied by a change of the solution color to orange. The stirring was continued for 3 hours at 40-30°C, The reactions are as follows (Y. Shan *et al*, 2014):



The samples were taken at different time intervals (1h, 2h and 3h) and characterized by X-ray diffraction (XRD) spectra that carried out by using a XRD-6000 Labx, supplied by SHIMADZU, X-ray source is Cu K α X-ray diffract-meter with radiation ($\lambda=1.5406 \text{ \AA}$). Scanning Electron Microscope studies were used to determine the nanoparticles distribution, nanoparticles size and show the structure and shape of nanocrystals using VEGA3 TESCAN, mode SE from TESCAN ORSAY HOLDING, a.s, Czech Republic. The UV-visible absorption spectrum of the prepared CdTe, measured using Shimadzu UV-1800 spectrophotometer. The energy gap of the prepared nanoparticles obtained from the relation (S. Saha and S.R. Bera, 2013):

$$(\alpha h\nu)^2 = C (h\nu - \Delta E_g), \text{ Where } C \text{ is constant.}$$

N-type Si wafer of (1.5 Ω .cm) resistivity and thickness was (508 \pm 15 μm) was used as a starting material in the photochemical etching in order to fabricate CdTe photoconductive detector. The samples were cut from the wafer and rinsed with acetone and methanol to remove dirt. In order to remove the native oxide layer on the samples, they were etched in diluted (10 %) HF Acid. After cleaning the samples they were immersed in HF acid of 50 % concentration and ethanol (1:1) in a Teflon beaker. Tungsten halogen lamp of 250 Watts integral with the dichroic ellipsoidal mirror was used as the photon beam source. The photoetching irradiation time was chosen to be 10 minutes. At the end of the photochemical etching process, the samples were rinsed with ethanol and stored in a glass containers filled with methanol to avoid the formation of oxide layer above the porous substrate.

CdTe film deposited on porous silicon by drops casting technique, and then annealed in vacuum with heating (400°C) for one hour. Micro mask of (0.4mm) electrode spacing was used to deposit the Al electrical electrodes on the film surface.

3. Results

The CdTe nanoparticles samples dried on quartz substrates. The position of all the diffraction peaks

matches well those of the bulk CdTe peaks in the PCPDFWIN data (CAS No.1306-25-8), as shown in Figure 1. These peaks are comparatively wider than that of the bulk materials due to finite crystalline size as in the reports (S. Saha and S.R. Bera, 2013; Y. He *et al*, 2006; F.O. Silva *et al*, 2012) that prepared with different methods. It seems from figure 1, that the peaks get narrower when the crystal size up to microstructure at sample 3. Also, there is a new peak present at sample 2 ($hkl=101$) not found in sample 1 but sample 3 show new crystallizations in all peaks. The average particle size of crystallites calculated according to the Scherer's formula (A.K. Tiwari *et al*, 2013):

$$\tau = \frac{k\lambda}{\beta \cos \theta} \quad (1)$$

Where k is the shape factor that has typical value 0.9, λ is the X-ray wavelength, β is the line broadening at half the maximum intensity (FWHM) in radians, and θ is the Bragg angle; τ is the mean size of the ordered (crystalline) domains, which may be smaller or equal to the grain size. Average sizes of crystallite calculated from Debye Scherer equation, are (7.2, 14, 32.4 nm), respectively for CdTe nanoparticles.

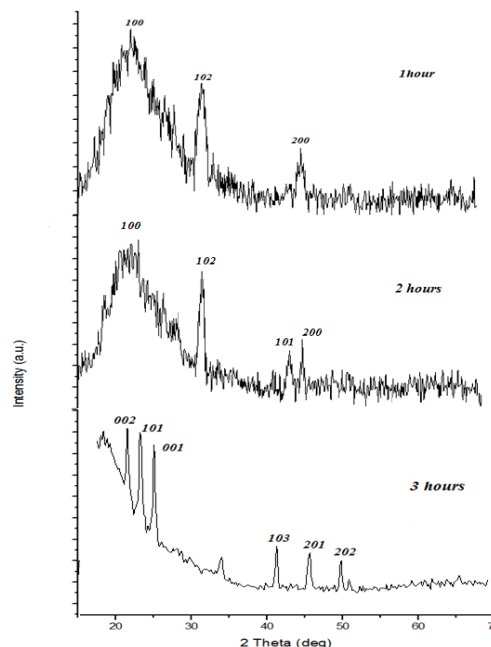
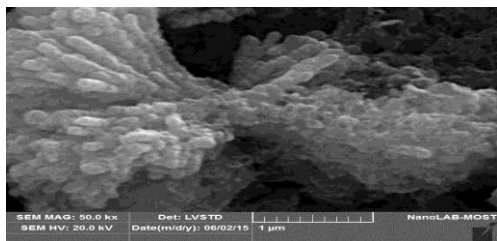


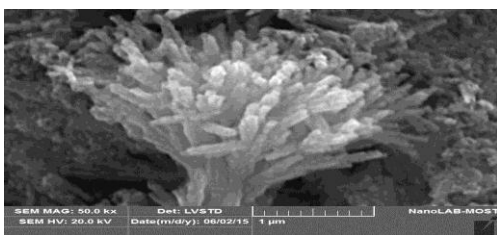
Fig: 1 The X-ray diffraction pattern of CdTe nanoparticles

Figure 2 shows a high magnification SEM image of the deposited CdTe samples on a glass substrate by drop casting method. These images show that the CdTe nanoparticles were flower of rods-like structures. The unequal film thickness due to deposition technique cause agglomerated particles and each nanorod seems to be stacked to other nanorods to form the flower like shape. There was an increase in particles size with increasing reaction time as shown in Table 1, the

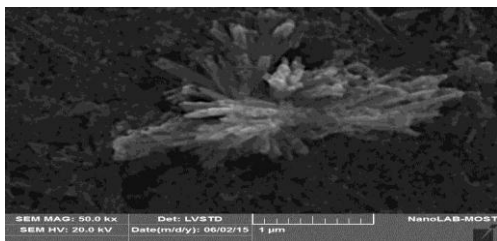
average dimensions (length and width) of CdTe nanorods evaluated from the SEM images using drawing scale, and the sample (3hour) had the largest average of nanorod width approaches the micrometer, while the average length of all nanorods were in microns.



(a) 1 hour



(b) 2 hours



(c) 3 hours

Fig: 2 SEM pictures of CdTe nanoparticles synthesized by aqueous chemical way for 3 hours of reaction time.

Table: 1 The Average Dimensions of CdTe nanorods

Reaction time period	Average Length of nanorods (μm)	Average Width of nanorods (nm)
1 hour	1.7087	80.6
2 hours	1.695	93.7
3 hours	0.9454	103.8

Figure 3 shows the absorption spectrum of CdTe nanoparticles in suspend, it reflects wide absorption range in the visible spectrum unlike the bulk material which have step absorption edges at 840 nm (X.N. Wang *et al*, 2010; E.R. Shaaban *et al*, 2014) and the absorption for CdTe nanoparticles increases monotonically with decreasing wavelength towards the UV. Also, the absorption peaks for CdTe are shifted toward the longer wavelength (red shift) with increasing time as well as increasing size of

nanoparticles as a consequence of the quantum confinement as proved in the reports (A.A. Ruth and J.A. Young, 2006; S. Ananthakumar *et al*, 2014; Y. Wang *et al*, 2013) that synthesized Nano CdTe with different ways.

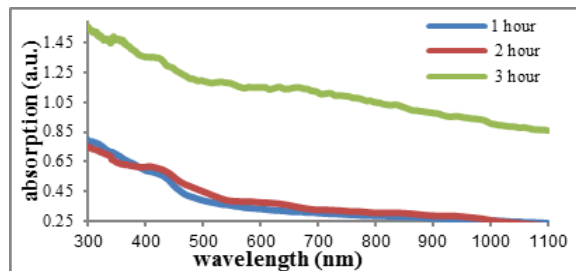


Fig: 3 The optical absorption spectrum of CdTe nanoparticles dispersed in distilled water generated by aqueous chemical method.

The energy gap for each reaction time for the prepared nanoparticles determined as shown in Figure 4.

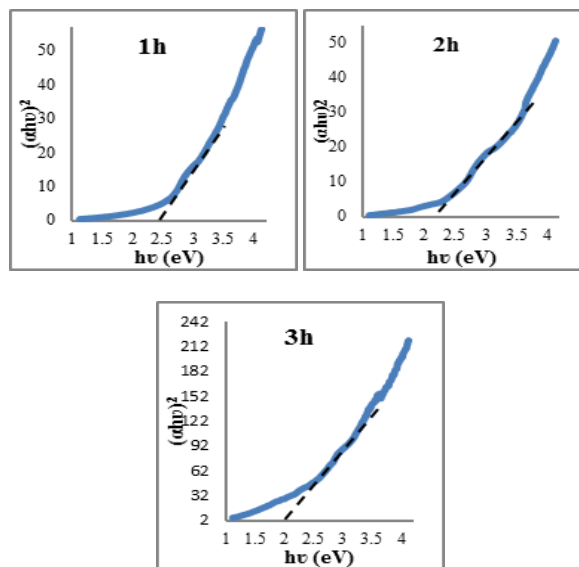


Fig: 4 Plot of $(\alpha h\nu)^2$ verses Energy ($h\nu$) to determine energy band gap for each reaction time period.

It is shown that the energy gap decreases with time approximately (2.4, 2.3, 2.1 eV) respectively which prove that the particle size increases with time.

The electrical properties of the prepared films were estimated from Hall measurements as shown in Table 2. These results shows that the mobility decreased with time of reaction due to the multiplicity in crystalline modes as shown in the XRD measurements which increase the grain boundaries in the nanoparticle that retard the charge movement also we see that the bulk concentration has increased with time with increasing the modes of crystallizations where more boundaries more defects then more charge carriers.

Table: 2 Hall parameters of CdTe nanoparticles thin films on glass substrates

Time duration	Resistivity (ρ) ($\Omega.cm$)	Conductivity (σ) ($1/\Omega.cm$)	Bulk concentration ($1/cm^3$)	Hall coefficient (R_H) (m^2/C)	Mobility (μ) ($cm^2/V.s$)
1h	1.086×10^5	9.207×10^{-6}	7.046×10^{10}	8.859×10^7	8.157×10^2
2h	1.65×10^5	6.06×10^{-6}	1.793×10^{11}	3.482×10^7	2.11×10^2
3h	1.567×10^5	6.382×10^{-6}	3.17×10^{11}	1.969×10^7	1.257×10^2

The variation of photoresponsivity of CdTe /PS Photoconductive visible detector with the bias voltage was carried out under the illumination with a Tungsten Halogen lamp 250Watt power. The operation circuit diagram of the detector (Figure 5). The current-voltage (I-V) characteristic of CdTe photoconductive detector for different time period (1, 2, 3 h) with the forward and reverse bias voltage at dark and under the illumination a Tungsten Halogen lamp is illustrated in Figure 6.

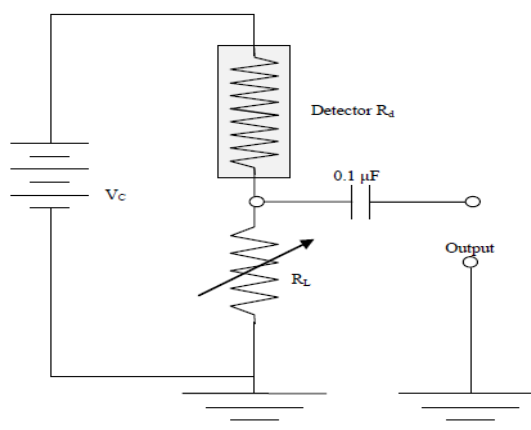


Fig: 5 The operation circuit diagram of CdTe photoconductive detector where; R_d is the detector element, R_L is the load resistance and V_C is the bias voltage (H.A. Thjeel *et al*, 2011)

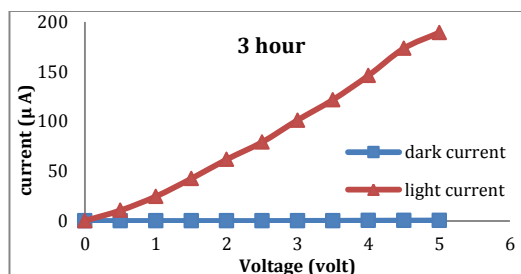
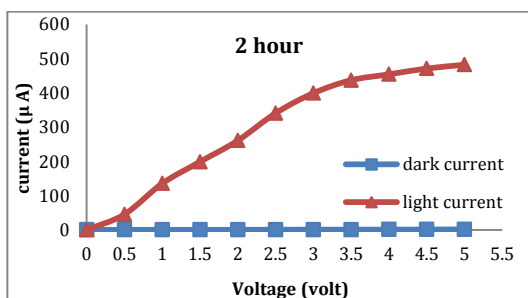
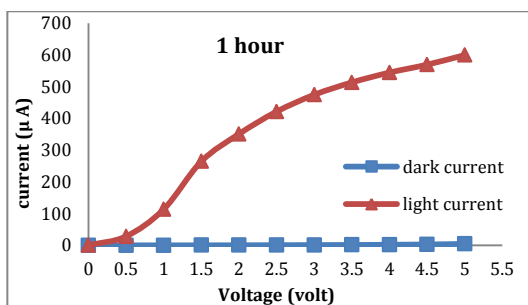


Fig: 6 I-V characteristic of CdTe photoconductive detector illuminated by Tungsten Halogen lamp for reaction time (1, 2, and 3h)

The device is used up to 5 V as a bias voltage and the corresponding current shows to be in microampere. It can be observed that the dark current is very low under dark, whereas the photocurrent is highly increased under the illumination by tungsten Halogen lamp. However, the photocurrent of the 1hour reaction time sample has the highest value; it might due to the smaller particle size of CdTe nanorods that led to high absorption and high number of photocarriers.

The measured photoelectric current gain (G) is a function of the electrode geometry from the relation:

$$G = \frac{\tau \mu v}{l^2} \tag{1}$$

(H.A. Thjeel *et al*, 2011),

Where τ is the carrier lifetime, μ is the charge carrier mobility, v is the applied voltage and l is the distance between the electrodes (0.04cm). This photoelectric current gain also, could be given by the equation:

$$G = \frac{I_{photo}}{I_{dark}} \tag{2}$$

(H.A. Thjeel *et al*, 2011),

Where I_{photo} is the light current and I_{dark} is the dark current which can be obtained from the I- V relation at fixed applied voltage (5 Volt), so from these two equations the carrier life time calculated. The detector resonsivity (R_λ) can be determined from the equation:

$$R_\lambda = \frac{I_{photo}}{power_{in}} \tag{3}$$

(S.M. Sze and Kwok K.Ng, 2007).

The other detector performance characteristic is the noise equivalent power (NEP) which is given by the following equation 4.

Table 3: figure of merit the photodetector parameters

Sample reaction time	Gain (G)	Response time (τ) (μ s)	Responsivity (R_λ)(A/Watt)	NEP (Watt)	Detectivity (D) (1/Watt)	Specific detectivity (D^*) ($\text{cm.Hz}^{1/2}.\text{W}^{-1}$)
1 h	133.11	52.2	0.617	$1.94 \cdot 10^{-12}$	$5.14 \cdot 10^{11}$	$5.14 \cdot 10^{11}$
2 h	301.25	456.6	0.496	$1.44 \cdot 10^{-12}$	$6.94 \cdot 10^{11}$	$6.94 \cdot 10^{11}$
3 h	378.6	963.5	0.195	$2.05 \cdot 10^{-12}$	$4.87 \cdot 10^{11}$	$4.87 \cdot 10^{11}$

$$NEP = \left(\frac{2e \cdot I_{dark} \cdot \Delta f}{R_\lambda} \right)^{1/2} \tag{4}$$

(S.M. Sze and Kwok K.Ng, 2007),

where e is the electron's charge ($1.6 \cdot 10^{-19}$) and Δf is electrical bandwidth equal to 1 HZ. The detector detectivity (D) is equal to the reciprocal of NEP, but the spesific detectivity (D^*) or called the normalized etectivity depends on the detectivity (D), the detector's area (A) 1cm^2 and the electrical band width Δf as follow:

$$D^* = D (A \cdot \Delta f)^{1/2} \tag{5}$$

(S.M. Sze and Kwok K.Ng, 2007)

Table 3 represents the results from the equations above.

It can be shown that the gain and the carrier life time (τ) or response time increases with increasing reaction time. In general, the presence of deep traps (pores in porous Si) in the semiconductor active layer causes a long carrier recombination lifetime for one type of charge, resulting in a high photoconductive gain because the gain is determined by the ratio of recombination lifetime and transit time for the carrier charges to sweep across the device. However, a long charge-trapping lifetime (or recombination lifetime) inevitably leads to a long device response time, which limits their applications (H. Wei *et al*, 2015). The responsivity decreases with reaction time (i.e. with increasing particle size) but the detectivity almost not rather changed with reaction time.

The trace of the output pulse on PC connected to voltmeter within the detector circuit is illustrated in Figure 6. It can be noticed from the traced signal that the rise time (10% - 90%) was of the order of (s) and the fall time (90% - 10%) was about (s) respectively (Table 4).

Table: 4 The rise and fall time for CdTe nanorods photodetector

Sample no.	Rise time (s)	Fall time (s)
1h	0.8	0.72
2h	0.7	0.8
3h	0.9	0.75

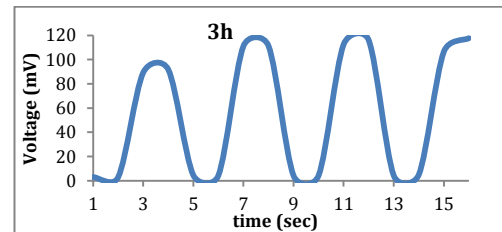
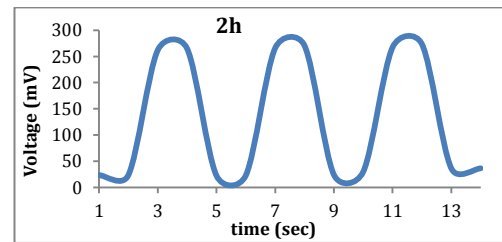
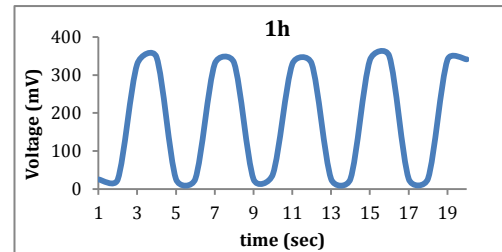


Fig: 6 The output pulse on PC connected to detector circuit

The long rise and fall (decay) times of CdTe nanorods (compared to very fast response photodetector) are attributed to the fact that the trapping and untrapping rates are much slower than the rate of the carrier recombination process. After the light source is cut off, the photocurrent still exists and the carriers do not sweep out of the device for some time. These carriers are stationary holes and yet to recombine, make the photocurrent remain after the light source is off. There is a trade-off between the response time and gain. Importantly, the existence of traps could prolong the carrier lifetime by destroying the electron-hole recombination and deterioration of time response but on the other hand this could result in enhanced responsivity and photoconductive gain in photodetectors (M. Shaygan *et al*, 2014).

Conclusion

CdTe nanorods visible photoconductive detector was successfully prepared on porous silicon with different reaction time. The result shows that the gain and

response time increases with increasing reaction time, whereas the responsivity decreases with reaction time (i.e. with increasing particle size).

Acknowledgment

The authors acknowledge prof. Abdulla M. Suhail from Dijlah College, Iraq and Dr. Rawa K.Ibrahim from Ministry of Science and Technology, Iraq for their advices.

References

- A.A. Ruth; J.A. Young (2006), Generation of CdSe and CdTe nanoparticles by laser ablation in liquids, *Colloids and Surfaces A: Physicochemical and Engineering Aspects*, vol.279, pp. 121-127.
- A.K. Tiwari; V.K. Verma; T.A. Jain; P.K. Bajpai (2013), Conclusive growth of CdTe nanorods by solvothermal decomposition using single source precursors, *Soft Nanoscience Letters*, vol.3, pp.52-57.
- A.L. Rogach (2000), Nanocrystalline CdTe and CdTe(S) particles: wet chemical preparation, size-dependent optical properties and perspectives of optoelectronic applications, *Materials Science and Engineering*, vol.B69, pp.435-440.
- D.V. Talapin; A.L. Rogach; I. Mekis; S. Haubold; A. Kornowski; M. Hasse; H. Weller (2002), Synthesis and surface modification of amino-stabilized CdSe, CdTe and InP nanocrystals, *Colloids and Surfaces A: Physicochemical and Engineering Aspects*, vol.202, pp.145-154.
- E.R. Shaaban; I.S. Yahia; N. Afify; G.F. Salem; W. Dobrowski (2014), Structural and the optical dispersion parameters of nano-CdTe thin film/flexible substrate, *Materials Science in Semiconductor Processing*, vol.19, pp.107-113.
- F.O. Silva; M.S. Carvalho; R. Mendonca; W.A. Macedo; K. Balzuweit; P. Reiss; M.A. Schiavon (2012), Effect of surface ligands on the optical properties of aqueous soluble CdTe quantum dots, *Nanoscale Research Letters*, vol.7, pp.536.
- H.A. Thjeel; A.M. Suhail; A.N. Naji; Q.G. Al-Zaidi; G.S. Muhammed; F.A. Naum (2011), Fabrication and Characteristics of Fast Photo Response ZnO/Porous Silicon UV Photoconductive Detector, *Advances in Materials Physics and Chemistry*, vol.1, pp.70-77.
- H. Wei; Y. Fang; Y. Yuan; L. Shen; J. Huang (2015), Trap Engineering of CdTe Nanoparticle for High Gain, Fast Response, and Low Noise P3HT:CdTe Nanocomposite Photodetectors, *Advanced Materials*.
- M.C. Kum; B.Y. Yoo; Y.W. Rheem; K.N. Bozhilov; W. Chen; A. Mulchandani; N.V. Myung (2008), Synthesis and characterization of cadmium telluride nanowire, *Nanotechnology*, vol.19, no.325711, pp.7.
- M. Shaygan; K. Davami; N. Kheirabi; C.K. Baek; G. Cuniberti; M. Meyyappand; J. Lee (2014), Single-crystalline CdTe nanowire field effect transistors as nanowire-based photodetector, *Phys. Chem. Chem. Phys.*, vol.16, pp.22687.
- M.S. Abd El-sadek and S.M. Babu (2010), Growth and optical characterization of colloidal CdTe nanoparticles capped by a bifunctional molecule, *Physica B*, vol.405, pp.3279-3283.
- R.S. Kpadnis; S.B. Bansode; S.S. Kale; H.M. Pathan (2013), Nanocrystalline CdTe thin films by electrochemical synthesis, *Carbon-Science and Technology*, vol.5, no.1, pp.211-217.
- S. Ananthakumar; J. Ramkumar; S.M. Babu (2014), Facile synthesis and transformation of Te nanorods to CdTe nanoparticles, *Materials Science in Semiconductor Processing*, vol.27, pp.12-18.
- S.M. Sze, Kwok K.Ng (2007), *Physics of Semiconductor Devices*, John Wiley & Sons, Hoboken, New Jersey, 3rd Edition.
- S. Saha and S.R. Bera (2013), Growth and characterization of CdTe nanostructures grown by chemical reduction route, *International Journal of Metallurgical & Materials*, vol.3, no.1, pp.37-40.
- S. Suresh (2014), Investigation on electrical properties of cadmium telluride thin films by chemical bath decomposition technique, *Journal of Non-Oxide Glasses*, vol.6, no.3, pp.47-52.
- W. Wang; S. Banerjee; S. Jia; M.L. Steigerwald; I.P. Herman (2007), Ligand Control of Growth, Morphology, and Capping Structure of Colloidal CdSe Nanorods, *Chem. Mater.*, vol.19, pp.2573-2580.
- X. N. Wang; J. Wang; M. J. Zhou; H. Wang; X. D. Xiao; Q. Li (2010), CdTe nanorods formation via nanoparticle self-assembly by thermal chemistry method, *Journal of Crystal Growth*, vol.312, pp.2310-2314.
- Y. He; H. Lu; L. Sai; W. Lai; Q. Fan; L. Wang; W. Huang (2006), Synthesis of CdTe nanocrystals through program process of microwave irradiation, *J. Phys. Chem. B*, vol.110, pp.13352-13356.
- Y. Liu; W. Chen; A.G. Joly; Y. Wang; C. Pope; Y. Zhang; J. Bovin; P. Sherwood (2006), Comparison of Water-Soluble CdTe Nanoparticles Synthesized in Air and in Nitrogen, *J. Phys. Chem. B*, vol.10, pp.9a124.
- Y. Shan; Z. Xiao; Y. Chuan; H. Li; M. Yuan (2014), One -pot aqueous synthesis of cysteine-capped CdTe/CdS core-shell nanowires, *Journal of Nanoparticle Research*, vol.16, pp.1-11.
- Y. Volkov; S. Mitchell; D. Kelleher; N. Gaponik; Y.P. Rakovich; J.F. Donegan; A.L. Rogach (2005), Highly emissive nanowires grown from CdTe nanocrystals in a phosphate buffer solution, *Proc. of SPIE*, vol.5824.
- Y. Wang; R. Wang; S. Liu; K. Yang; L. Zhou; H. Li (2013), Synthesis and characterization of CdTe quantum dots by one step method, *Bull. Chem. Soc. Ethiop*, vol.27, pp.387-393.
- Y. Zhang and A. Clapp (2011), Overview of Stabilizing Ligands for Biocompatible Quantum Dot Nanocrystals, *Sensors*, vol.11, pp.11036-11055.